ChemistryOpen

Supporting Information

Polymer–Supported Liquid Layer Electrolyzer Enabled Electrochemical CO$_2$ Reduction to CO with High Energy Efficiency

Shangyu Li, Yiwen Ma, Tiancheng Zhao, Jiaxin Li, Xinyue Kang, Wen Guo, Yunzhou Wen, Liping Wang, Yurui Wang, Renxing Lin, Tiantian Li, Hairen Tan,* Huisheng Peng,* and Bo Zhang*

Reagents

Ethanol (≥99.5%) and potassium hydroxide (KOH, ≥85%) were purchased from Sinopharm. All the chemicals were used without further purification. Milli-Q grade water (18.2 MΩ) was used to prepare all solutions.

Electrode preparation

10 mg multi-walled carbon nanotubes (MWCNTs) reported in our previous work[1] were cut into pieces and dispersed into 20 mL ethanol by 2 hours stirring and ultrasonication. 200 mg Ag nanoparticles (<100 nm particle size, Sigma-Aldrich) were added to the dispersion and then underwent ultrasonic treatment for 1 hour. To produce the cathode, 2 mL dispersion was dropped onto 4 cm^2 commercially available gas diffusion layers (Sigracet 28BC, Fuel Cell Store) after adding 80 μL 5% Nafion solution (Sigma-Aldrich) and underwent ultrasonic treatment for another 30 minutes. NiFe-based anode was produced according to a previous report[2].

Electrode characterization

The morphologies of these catalysts were acquired using a Hitachi FE-SEM S-4800 scanning electron microscope (SEM) operated at 1.0 kV. High-resolution transmission electron microscopy (HRTEM) images were taken on a JEOL JEM-2100F transmission electron microscopy operated at 200 kV. X-ray photoelectron spectroscopy (XPS) was recorded on a PHI5300 instrument with Mg Kα X-ray sources. Powder X-ray diffraction (XRD) patterns were obtained with a MiniFlex600 instrument with Cu-Ka radiation (40 kV, l = 1.5406 Å) using a scan rate of $0.1° s^{-1}$.

Electrochemistry.

The electrolyzers used for electrochemical CO_2 reduction to CO were comprised by a series of polymethyl methacrylate plates and soft silicone pads (Fig. S1). Ag based cathode was fed with CO_2 (Shanghai TOMOE gases, 99.99%) and 6 M potassium hydroxide was fed to NiFe-based anode through a peristaltic pump, with an effective geometric area of 1 cm^2. Silicone pad acted as a seal to avoid leakage and ensure gas tightness, and Cu tapes were used as the current collector.

For the membrane-free liquid-phase electrolyzer, different polymethyl methacrylate plates and silicone pads were used to separate the anode and cathode, regulating the electrolyte layer thickness. For the polymer-supported liquid layer (PSL) electrolyzer, a piece of polypropylene non-woven fabric was used between the anode and cathode.

All the linear sweep voltammetry (LSV), steady-state chronopotentiometry, open-circuit potential, and AC electrochemical impedance spectroscopy (EIS) measurements were conducted using an electrochemical workstation (Autolab PGSTAT204) with a two-electrode setup, and EIS data were collected from 0.1 to 10^5 Hz at a cell voltage of 1.6 V with the amplitude of 10 mV. The Tafel slopes were tested by three-electrode system, in which the cathode was attached closely to the polypropylene non-woven

fabric, anion exchange membrane (AEM) or cation exchange membrane (CEM), and a HgO/Hg electrode was used as the reference electrode.

Products analysis

The gas products (CO, H_2) were analyzed online continuously by a gas chromatograph (Ruimin Technologies, GC2060). The gas chromatograph was equipped with a packed TDX-01 column, a packed 5A column and Porapak T column. Nitrogen (Shanghai TOMOE gases, 99.999%) was used as the carrier gas. CO was converted to CH_4 in a Nickel catalyst kit and then quantified *via* a flame ionization detector (FID), and H_2 concentration was quantified *via* a thermal conductivity detector (TCD). The gas chromatography was calibrated by certified standard gases in advance, and the faradaic efficiencies (FE) of products were calculated as follows:

$$FE = \frac{\varphi v}{j} \frac{PnF}{RT} \times 100\%$$

where φ is the volume fraction of CO or H_2, v represents the CO_2 gas flow rate, and j is the total current from the potentiostat. P, n, F, R, and T are pressure, number of electrons transferred, Faradaic constant, ideal gas constant and temperature, respectively.

All-perovskite monolithic tandem cell fabrication

The tandem cells were fabricated according to previous works[3]. The NiO nanocrystals (25 mg ml^{-1}) and VNPB (0.5 mg ml^{-1}) were deposited on the cleaned ITO substrate successively by spin coating, which served as the hole transport layer of the wide-bandgap subcell. Wide-bandgap perovskite films with a composition of $FA_{0.8}Cs_{0.2}Pb(I_{0.62}Br_{0.38})$ were deposited on top of VNPB-modified NiO with a two-step spin-coating procedure: (1) 2,000 r.p.m. for 10 s with a ramp-up of 200 r.p.m. s^{-1} and (2) 6,000 r.p.m. for 40 s with an acceleration of 2,000 r.p.m. s^{-1}. 150 µl chlorobenzene was dropped on the spinning substrate during the second spin-coating step at 20 s before the end of the procedure. The substrate was then annealed on a hot plate at 100 °C for 15 minutes. After cooling to room temperature, a 20-nm-thick C_{60} film was subsequently deposited on top by thermal evaporation. The substrates were then transferred to the ALD system (Veeco Savannah S200) to deposit 20 nm SnO_2 at low temperatures using precursors of tetrakis (dimethylamino) tin(iv) (99.9999%, Nanjing Ai Mou Yuan Scientific Equipment) and deionized water. After ALD deposition, a thin layer of Au (~1 nm) was deposited on ALD-SnO_2 by thermal evaporation. PEDOT-PSS layers were spin-cast on top of SnO_2-protected front cells and annealed in air at 120 °C for 20 min. After the substrates had cooled, we immediately transferred the substrates to a nitrogen-filled glovebox. Narrow-bandgap perovskite films with a composition of $FA_{0.7}MA_{0.3}Pb_{0.5}Sn_{0.5}I_3$ were deposited on top of PEDOT: PSS with a two-step spin-coating procedure: (1) 1,000 r.p.m. for 10 s with an acceleration of 200 r.p.m. s^{-1} and (2) 4,000 r.p.m. for 40 s with a ramp-up of 1,000 r.p.m. s^{-1}. 300 µl ethyl acetate was dropped on the spinning substrate during the second spin-coating step at 20 s before the end of the procedure. Tin powders and formamidine sulfinic acid (0.3 mol%) were added in the precursor solution. The substrates were then transferred onto a hotplate and heated at 100 °C for 10 min. After cooling to room temperature, the

substrates were transferred to the evaporation system. Finally, 20-nm-thick C_{60}, 7-nm-thick-BCP and 100-nm-thick Cu were sequentially deposited on top of the perovskite by thermal evaporation.
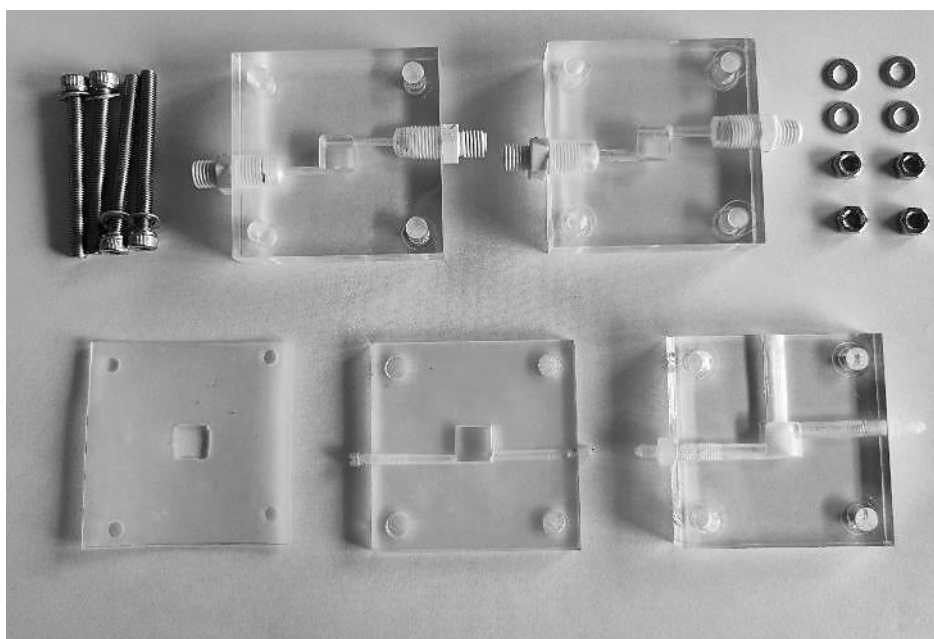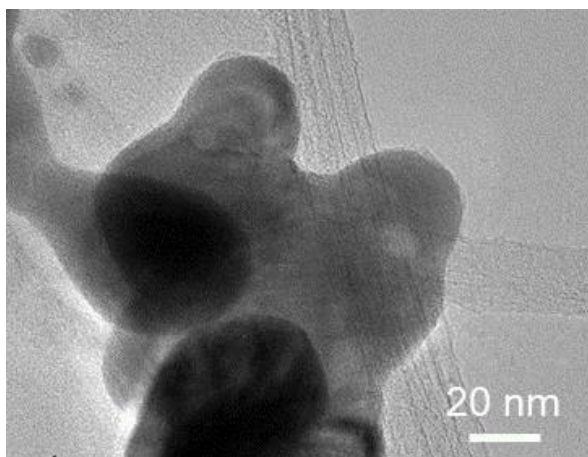
Supporting Figure 1 | Photograph of polymethyl methacrylate plates with different thicknesses and silicone pads used for electrolyzers.
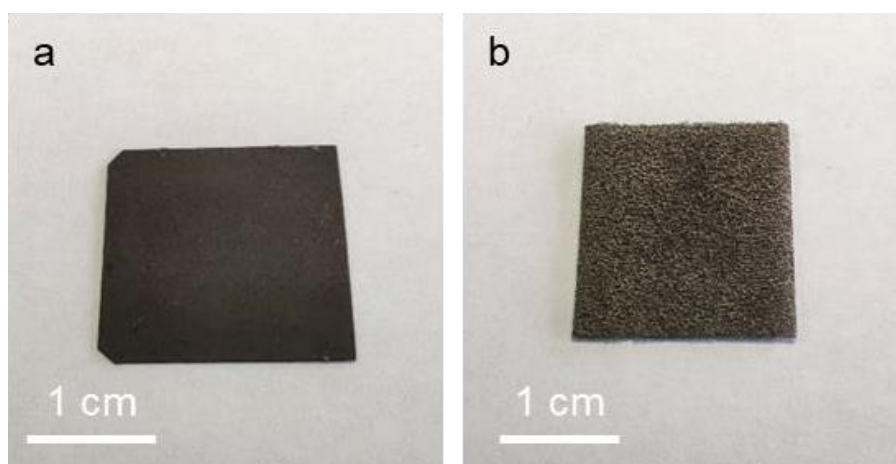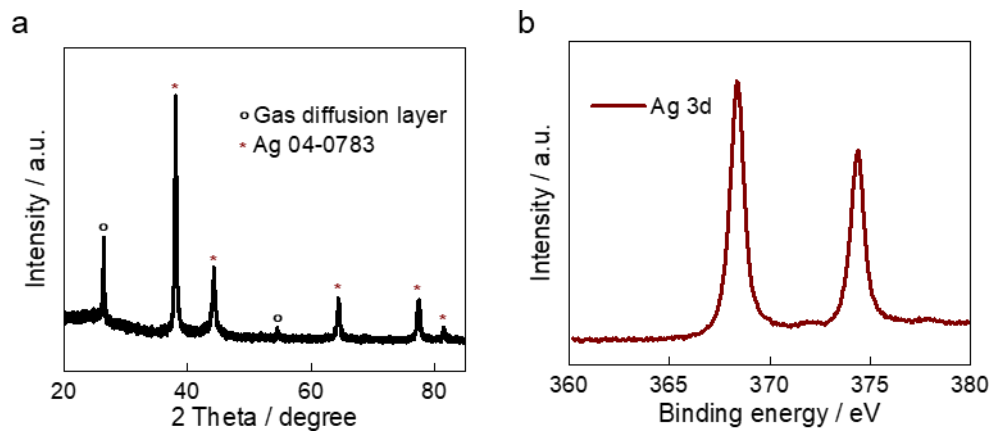
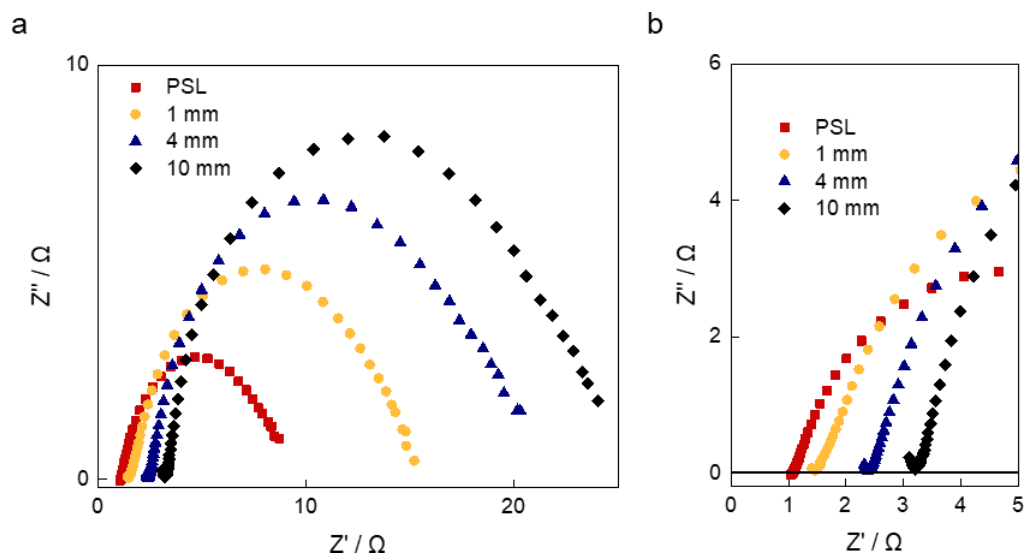**Supporting Figure 2 |** Photographs of (a) Ag-based cathode, (b) NiFe-based anode.
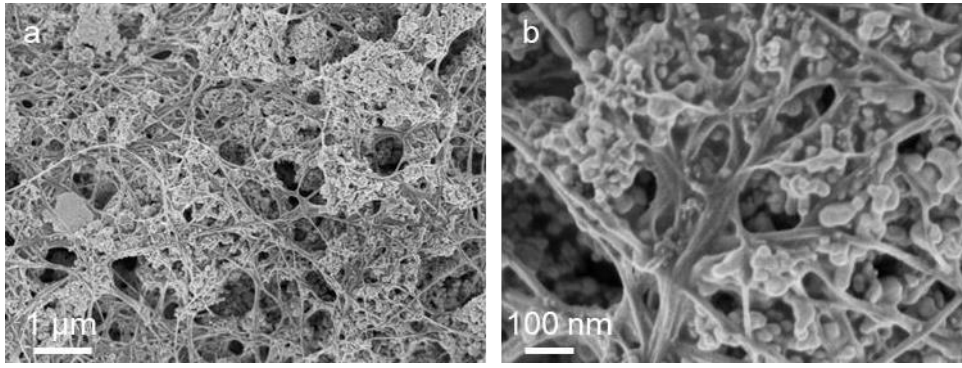
**Supporting Figure 3 |** SEM images of Ag-based cathode at (a) low and (b) high resolutions.

**Supporting Figure 4 |** TEM image of homemade Ag-based catalyst.

Supporting Figure 5 | (a) XRD pattern and (b) XPS spectra of Ag based catalyst.

Supporting Figure 6 | (a) Nyquist diagram of PSL electrolyzer and liquid-phase electrolyzers with different electrolyte layer thicknesses at a constant cell voltage of 1.6 V. (b) Magnified spectra of the high frequency region.
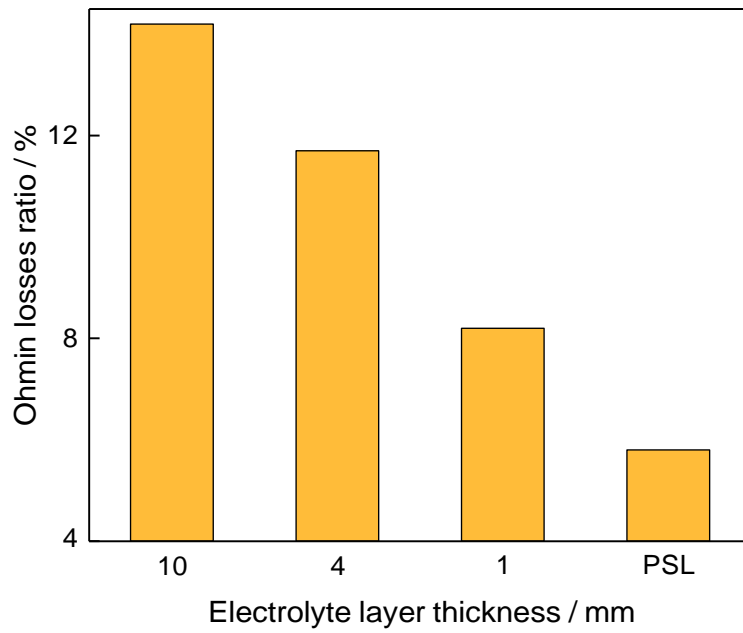
Supporting Figure 7 | Ratio of ohmic losses in full cell voltage of PSL and liquid-phase electrolyzers with different electrolyte layer thicknesses at 100 mA cm^{-2}.
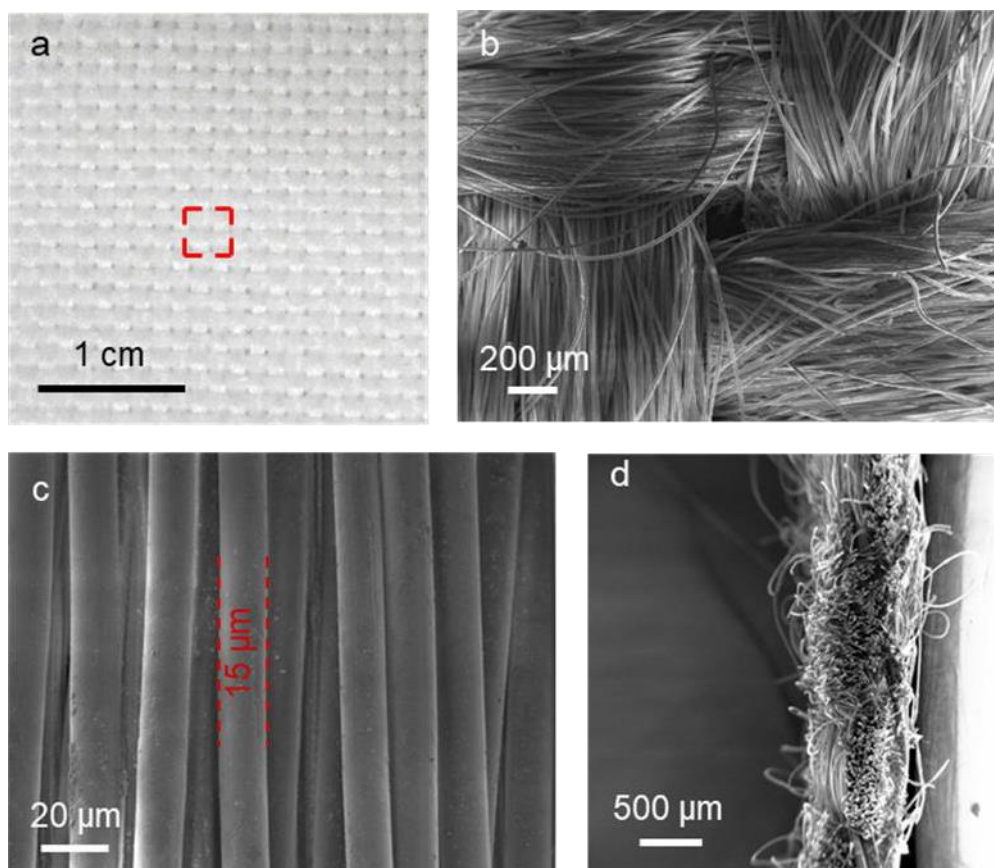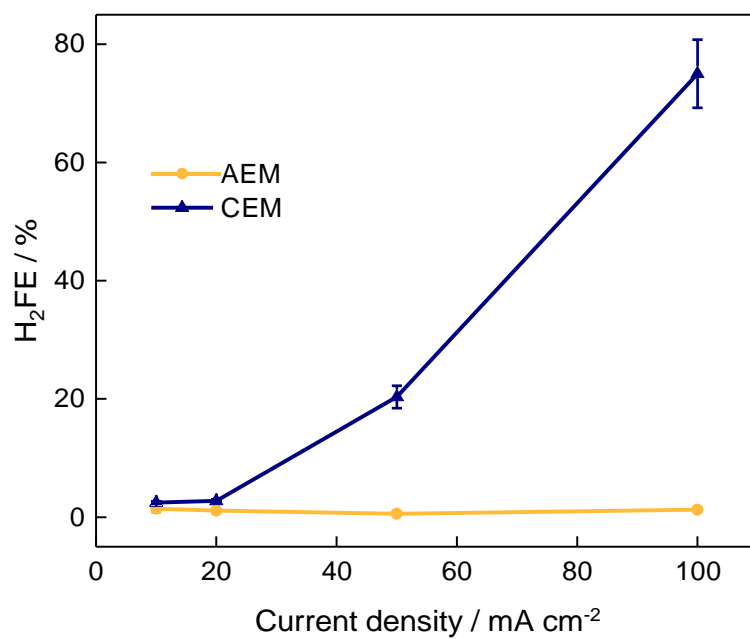
Supporting Figure 8 | (a) Photograph of the polypropylene non-woven fabric. SEM images of the polypropylene non-woven fabric by (b) top view, (c) enlarged top view and (d) cross-sectional view.
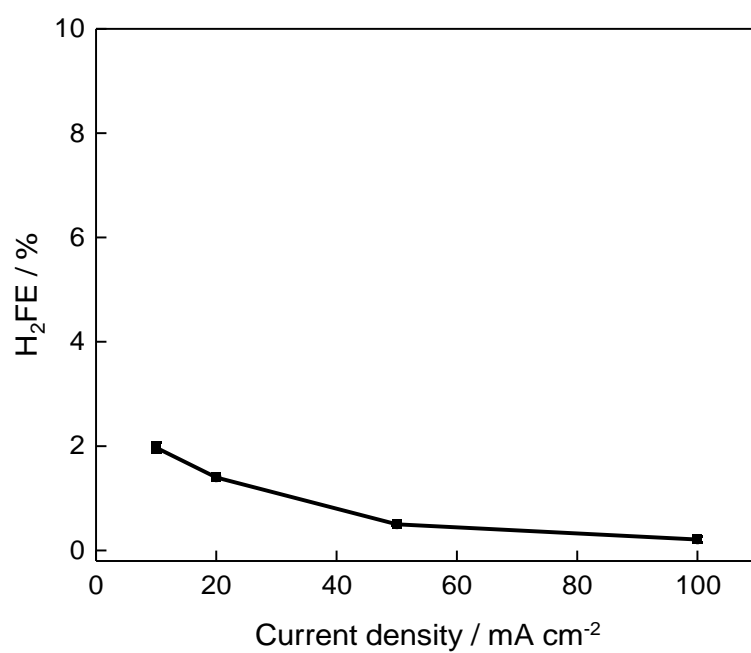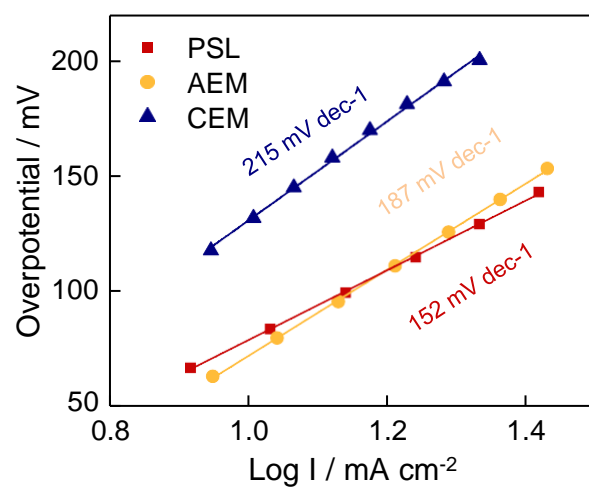
Supporting Figure 9 | H$_2$FE of PSL electrolyzer at different current densities.
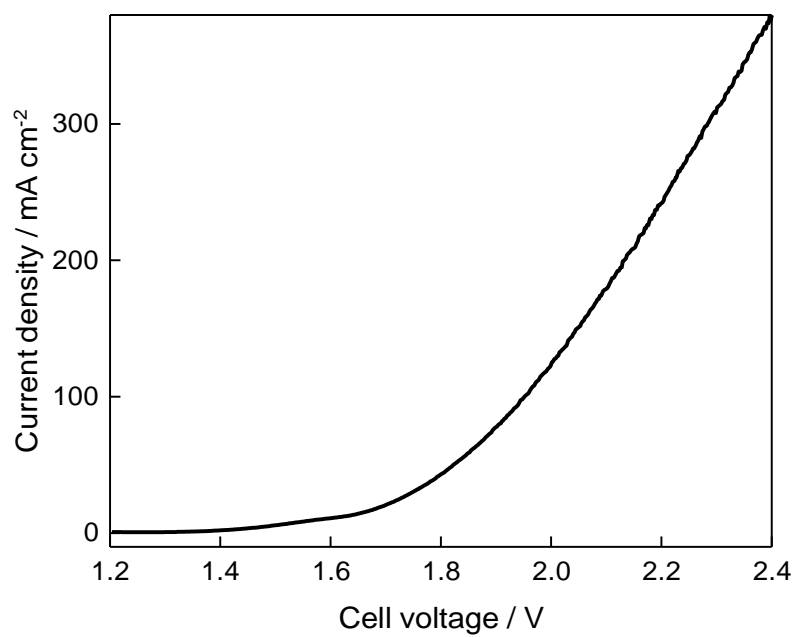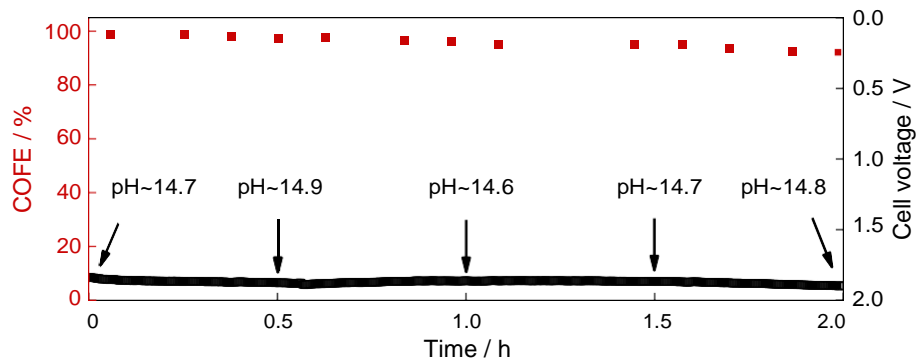
Supporting Figure 10 | Linear sweep voltammogram curve of PSL electrolyzer at a scan rate of 10 mV s^{-1}.

Supporting Figure 11 | H_2FE of AEM and CEM electrolyzers at different current densities.

Supporting Figure 12 | The Tafel slopes of eCO₂R in PSL, AEM and CEM structure.

Supporting Figure 13 | The anolyte pH, COFE and cell voltage versus time for the PSL electrolyzer working at the current density of 50 mA cm^{-2}.

Supporting Figure 14 | Photograph of the all-perovskite monolithic tandem photovoltaic cell with an active area of 1 cm^2.

Table S1. Parameters of the polypropylene non-woven fabric.

diaphragm	Thickness [mm]	Puncture strength[a] [MPa]	Wettability[b] [mg cm^{-2}]
Polypropylene non-woven fabric	0.6	15.3±1.9	77.1±5.3

[a] The puncture strength was tested by a universal tensile tester. In order to better match the conditions in the assembly process of the electrolyzer, the diameter of the test probe was 0.5 mm and the test speed was 50 mm min^{-1}.[4]

[b] In order to better measure the electrolyte uptake ability of the diaphragms, we used the mass changes before and after diaphragms infiltration of electrolyte to characterize the wettability.[5]

References for the Supporting Information

[1]   L. Ye, M. Liao, T. Zhao, H. Sun, Y. Zhao, X. Sun, B. Wang, H. Peng, *Angew. Chem. Int. Ed.* **2019**, *58*, 17054-17060.
[2]   B. Fei, Z. Chen, J. Liu, H. Xu, X. Yan, H. Qing, M. Chen, R. Wu, *Adv. Energy Mater.* **2020**, *10*, 2001963.
[3]   a) K. Xiao, R. Lin, Q. Han, Y. Hou, Z. Qin, H. T. Nguyen, J. Wen, M. Wei, V. Yeddu, M. I. Saidaminov, Y. Gao, X. Luo, Y. Wang, H. Gao, C. Zhang, J. Xu, J. Zhu, E. H. Sargent, H. Tan, *Nat. Energy* **2020**, *5*, 870-880; b) R. Lin, K. Xiao, Z. Qin, Q. Han, C. Zhang, M. Wei, M. I. Saidaminov, Y. Gao, J. Xu, M. Xiao, A. Li, J. Zhu, E. H. Sargent, H. Tan, *Nat. Energy* **2019**, *4*, 864-873.
[4]   S. W. Kim, M. H. Ryou, Y. M. Lee, K. Y. Cho, *J. Alloys Compd.* **2016**, *675*, 341-347.
[5]   W. Chen, L. Shi, H. Zhou, J. Zhu, Z. Wang, X. Mao, M. Chi, L. Sun, S. Yuan, *ACS Sustainable Chem. Eng.* **2016**, *4*, 3794-3802.